# Hepatic uptake and metabolism of galactose can be quantified in vivo by 2-[ $^{18}$F]fluoro-2-deoxygalactose positron emission tomography

**Michael Sørensen, Ole Lajord Munk, Frank Viborg Mortensen, Aage Kristian Olsen, Dirk Bender, Ludvik Bass and Susanne Keiding**

*Am J Physiol Gastrointest Liver Physiol* 295:G27-G36, 2008. First published 15 May 2008; doi:10.1152/ajpgi.00004.2008



***AJP - Gastrointestinal and Liver Physiology*** publishes original articles pertaining to all aspects of research involving normal or abnormal function of the gastrointestinal tract, hepatobiliary system, and pancreas. It is published 12 times a year (monthly) by the American Physiological Society, 9650 Rockville Pike, Bethesda MD 20814-3991.  ISSN: 0193-1857, ESSN: 1522-1547. Visit our website at http://www.the-aps.org/.

*Am J Physiol Gastrointest Liver Physiol* 295: G27–G36, 2008.
First published May 15, 2008; doi:10.1152/ajpgi.00004.2008.

# Hepatic uptake and metabolism of galactose can be quantified in vivo by 2-[$^{18}$F]fluoro-2-deoxygalactose positron emission tomography

**Michael Sørensen,[1,2] Ole Lajord Munk,[1] Frank Viborg Mortensen,[3] Aage Kristian Olsen,[1] Dirk Bender,[1] Ludvik Bass,[4] and Susanne Keiding[1,2]**

[1]*PET Center,* [2]*Department of Medicine V, and* [3]*Department of Surgery L, Aarhus University Hospital, Aarhus, Denmark; and* [4]*Department of Mathematics, University of Queensland, Brisbane, Australia*

Submitted 3 January 2008; accepted in final form 14 May 2008

**Sørensen M, Munk OL, Mortensen FV, Olsen AK, Bender D, Bass L, Keiding S.** Hepatic uptake and metabolism of galactose can be quantified in vivo by 2-[$^{18}$F]fluoro-2-deoxygalactose positron emission tomography. *Am J Physiol Gastrointest Liver Physiol* 295: G27–G36, 2008. First published May 15, 2008; doi:10.1152/ajpgi.00004.2008.—Metabolism of galactose is a specialized liver function. The purpose of this PET study was to use the galactose analog 2-[$^{18}$F]fluoro-2-deoxygalactose (FDGal) to investigate hepatic uptake and metabolism of galactose in vivo. FDGal kinetics was studied in 10 anesthetized pigs at blood concentrations of nonradioactive galactose yielding approximately first-order kinetics (tracer only; $n = 4$), intermediate kinetics (0.5–0.6 mmol galactose/l blood; $n = 2$), and near-saturation kinetics (>3 mmol galactose/l blood; $n = 4$). All animals underwent liver $C^{15}O$ PET (blood volume) and FDGal PET (galactose kinetics) with arterial and portal venous blood sampling. Flow rates in the hepatic artery and the portal vein were measured by ultrasound transit-time flowmeters. The hepatic uptake and net metabolic clearance of FDGal were quantified by nonlinear and linear regression analyses. The initial extraction fraction of FDGal from blood-to-hepatocyte was unity in all pigs. Hepatic net metabolic clearance of FDGal, $K^{FDGal}$, was 332–481 ml blood·min$^{-1}$·l$^{-1}$ tissue in experiments with approximately first-order kinetics and 15.2–21.8 ml blood·min$^{-1}$·l$^{-1}$ tissue in experiments with near-saturation kinetics. Maximal hepatic removal rates of galactose were on average 600 μmol·min$^{-1}$·l$^{-1}$ tissue (range 412–702), which was in agreement with other studies. There was no significant difference between $K^{FDGal}$ calculated with use of the dual tracer input ($K^{FDGal}_{dual}$) or the single arterial input ($K^{FDGal}_{arterial}$). In conclusion, hepatic galactose kinetics can be quantified with the galactose analog FDGal. At near-saturated kinetics, the maximal hepatic removal rate of galactose can be calculated from the net metabolic clearance of FDGal and the blood concentration of galactose.

liver physiology; Michaelis-Menten kinetics; liver function; clearance; galactokinase

THE HEXOSE GALACTOSE IS ALMOST exclusively metabolized in the liver, a property that is utilized in the galactose elimination capacity test (GEC) (47, 48). The GEC estimates the liver's maximal capacity for removing and metabolizing blood-borne galactose, and this reflects how well the individual liver functions. The clinical value of the GEC as a prognostic marker in patients with liver disease is well documented (15, 16, 20, 34, 35, 41, 43). Galactose kinetics and metabolism are therefore of great interest for hepatologists and have been studied thoroughly. Studies have shown that galactose enters hepatocytes freely from the blood (11) and that the first step in intracellular metabolism of galactose is phosphorylation to galactose-1-phosphate (17), a reaction catalyzed by the galactokinase enzyme. This phosphorylation has furthermore been shown to be the rate-limiting step in hepatic metabolism of galactose and follows Michaelis-Menten saturation kinetics in vivo (22, 29). The GEC test thus reflects the total in vivo activity of the galactokinase enzyme.

Previous studies of galactose metabolism have been carried out in purified enzymes (2, 3, 46, 49), isolated perfused rat livers (24, 25, 44), dog livers (11), isolated perfused pig livers (22, 23, 28), anesthetized pigs (26, 51), and human subjects (47, 48, 27, 32, 42). So far, all in vivo studies have been based on measurements of galactose concentrations in arterial blood and in some cases supplemented with liver vein blood samples. Such studies yield information on the net uptake of galactose across the whole liver but not of specific rate constants for hepatic uptake and metabolism of galactose. Advanced PET technology has now made this feasible (45). The galactose analog 2-deoxygalactose has been labeled with $^{18}$F, forming 2-[$^{18}$F]fluoro-2-deoxygalactose (FDGal), which is detectable by a PET camera (9, 12, 19). External detection by PET of the time-dependent distribution of FDGal in tissue following an intravenous (IV) injection makes it possible to estimate specific rate constants for hepatic uptake and metabolism in vivo (45). No such PET studies of FDGal kinetics in the liver have yet been published although PET studies of rodents have shown that radioactivity following an IV infusion of FDGal accumulates very specifically in the liver (9, 12, 19). The liver's special dual blood supply from the hepatic artery (HA) and the portal vein (PV) has been the main obstacle for more detailed studies (9). The special arrangement of the liver between the PV drained viscera and the systemic blood circulation makes it difficult to calculate the correct flow-weighted dual input, viz. the mixed arterial-portal input. Since PV catheterization is not possible in humans, animals are suitable for such studies. In recent years this has been utilized in studies of other tracer kinetics such as the sugar analog 2-[$^{18}$F]fluoro-2-deoxyglucose (FDG) (18, 36). These studies have shown that the hepatic net metabolic clearance of FDG during quasi-steady-state metabolism can be calculated by linear representation of dynamic PET data and the single arterial input (18, 36).

The aim of the present in vivo PET study in pigs was to evaluate the feasibility of using FDGal as a PET tracer in studies of hepatic galactose metabolism and to gain new insight into galactose kinetics. We used the anesthetized pig model,

Address for reprint requests and other correspondence: M. Sørensen, PET Center, Aarhus Univ. Hospital, DK-8000 Aarhus, Denmark (e-mail: michael@pet.auh.dk).

The costs of publication of this article were defrayed in part by the payment of page charges. The article must therefore be hereby marked "*advertisement*" in accordance with 18 U.S.C. Section 1734 solely to indicate this fact.

which has the advantage that blood sampling from the PV is possible. This gives us the opportunity to determine the mixed arterial-portal input, i.e., the dual input. Furthermore, the metabolism of the pig liver resembles that of the human liver very closely. Our setup allowed us to estimate specific kinetic parameters for transport from blood to hepatocyte and the subsequent intracellular metabolism of FDGal. We also studied the importance of using the liver's dual input in the estimation of the net metabolic clearance of FDGal vs. using the single arterial input. If the net metabolic clearance of galactose can be quantified using dynamic FDGal PET and the single arterial input, this makes the method applicable for human studies.

## MATERIALS AND METHODS

*Study design.* $^{15}$O-CO (CO) and FDGal PET studies were performed after preparation of the animals. CO PET was used to determine the vascular volume of the liver. After decay of this tracer (10 min), a 90-min dynamic PET recording was performed with an IV injection of 200 MBq FDGal during the initial 15 s. Kinetic parameters for uptake and metabolism of FDGal were determined by nonlinear regression analysis and by graphical analysis (linear representation) of data. Individual steady-state blood concentrations of galactose were reached by means of a constant IV infusion of galactose or saline. This resulted in experiments with FDGal kinetics ranging from approximately first-order kinetics (with only tracer amounts of FDGal in blood; $n = 4$), intermediate kinetics (blood concentrations of galactose 0.49 and 0.62 mmol/l; $n = 2$) to approximately zero-order (near-saturation) kinetics (blood concentration of galactose >3 mmol/l; $n = 4$). Because of the long radioactive half-life of FDGal (109 min), only one FDGal PET study could be performed in each animal.

All experiments were approved by the Danish Ministry of Legal Affairs and performed in accordance with European Union, nationally, and institutionally approved guidelines for animal welfare.

*Animals and animal preparations.* Ten female pigs (Yorkshire × Danish Landrace; body wt 36.5–40.5 kg) were fasted for 16 h with free access to water. Just before surgery, the animal was premedicated with an intramuscular injection of 50 mg midazolam +250 mg S-ketamine. Anesthesia was induced by an intravenous injection of 50 mg midazolam +125 mg S-ketamine via a cannula in an ear vein and maintained by a constant IV infusion of 300 mg propofol, 250 mg S-ketamine, and 50 mg midazolam in 50 ml (40 ml/h). The animal was intubated and ventilated by mechanical respiration (Hallowell EMC model 2000 respirator).

The left femoral artery and vein were exposed, and Avanti catheters (Cordis) were inserted into both vessels. After interdigital reflexes were checked to secure sufficiently deep anesthesia, 4 mg pancuronium was injected IV. The abdomen was opened through a 30-cm-long subcostal incision below the right curvature and the hepatoduodenal ligament was identified. The common bile duct, the HA and the PV were exposed and ultrasound transit-time flowmeters (CardioMed; In vivo Aps, Oslo, Norway) placed around the two blood vessels for flow measurements. A 5.3-F polyethylene catheter (William Cook Europe) was inserted into the PV for blood sampling. It was placed downstream to the flowmeter in order not to disturb flow measurements. Finally, the surgical incision was closed and catheters and lines of the flowmeters were secured to the abdominal surface to avoid displacement.

Six of the pigs received an intravenous injection of 70 mmol galactose (Kabi, Sweden) in 50 ml of isotonic saline (0.9% NaCl) followed by a constant IV infusion of a galactose solution with concentrations ranging from 139 to 348 μmol galactose/l isotonic saline (infusion rate was 216 ml/h). The infusion was started 75–90 min prior to the PET study to allow for the galactose to distribute and reach a steady-state concentration in blood. The infusion was sustained throughout the study. Four pigs received an IV bolus of isotonic saline followed by a constant infusion of isotonic saline without galactose.

*PET recordings and blood sampling.* After abdominal surgery, the anesthetized pig was placed in a supine position with the liver within the 15-cm field of view of the PET camera (Siemens ECAT EXACT HR-47, CTI/Siemens Medical Systems, Knoxville, TN). A 5-min scan using a rotating external $^{68}$GE/$^{68}$GA rod was performed to ensure that the liver was in the center of the camera's field of view. After any necessary adjustments, a transmission scan of 15 min was performed for later attenuation correction of the emission recordings.

Two dynamic CO recordings were performed in each animal after inhalation of 1,000 MBq CO administered through the respirator to determine the vascular volume of the liver (36). Dual estimates from each pig deviated less than 5% from each other, and the individual mean value of the two estimates were accordingly used.

Ten minutes after the last CO recording we injected 200 MBq FDGal in 10 ml of saline through the catheter in the femoral vein during the initial 15 s of the dynamic PET recording. The FDGal protocol consisted of 52 time frames (18 × 5 s, 15 × 10 s, 4 × 30 s, 4 × 60 s, 6 × 300 s, and 5 × 600 s; total 90 min). FDGal was produced at the PET center's own radiochemistry laboratory according to the method described elsewhere (5).

Emission data were corrected for radioactive decay back to the start of the scan. All recordings were reconstructed in a Gaussian filtered backprojection mode with an attenuation based on the initial transmission scan. This resulted in three-dimensional images of 128 × 128 × 47 voxels with a size of 2.4 × 2.4 × 3.1 mm$^3$ and a central spatial resolution of 6.7 mm full width at half maximum.

During the FDGal PET recording, successive blood samples (0.5 ml) were drawn from the femoral artery and the PV at 18 × 5 s, 6 × 10 s, 3 × 20 s, 3 × 60 s, 1 × 120 s, 1 × 240 s, 1 × 360 s, and 7 × 600 s. Blood concentrations of radioactivity were measured with a well counter (Packard Instruments, Meriden, CT), corrected for radioactive decay back to start of the scan and blood concentrations of radioactivity over time [time-activity curves (TACs)] for portal venous and arterial blood were generated. In order not to disturb the flow in the HA during the study we withdrew arterial blood samples from the femoral artery, since the concentration of FDGal in the femoral artery is equal to that in the HA without any detectable time-delay.

The arterial blood concentration of galactose was determined enzymatically (31) three times during the FDGal PET recording.

Blood flow rates in the PV and the HA were recorded by the transit-time flowmeters every 10 s during the initial 3 min of the PET recording, then every 30 s for the next 2 min, at 5 and 10 min, and then every 10 min for the rest of the study period.

Arterial blood pressure values were monitored every 30 min throughout the experiment to ensure physiologically stable animals. By adjusting the mechanical respiration, we kept arterial $P_{CO_2}$, $P_{O_2}$, and pH between 3.5–7.0 kPa, 18.0–25.0 kPa, and 7.35–7.45, respectively. Blood glucose was between 5.0 and 6.7 mmol/l blood. Body temperature was kept between 38.5 and 39.5°C by adjusting an electric heating pad placed under the animal.

The experiment was ended by an IV injection of 4 g pentobarbital sodium. The liver was immediately removed and weighed (mean 909 g, range 790–1,048 g).

*FDGal metabolites in blood.* To investigate the possible appearance of FDGal metabolites in peripheral blood, we analyzed blood samples from two pigs at 1, 2, 3, 5, 9, 12, 18, 30, 40, 50, 60, 70, 80, and 90 min after injection of 200 MBq FDGal.

Plasma proteins were precipitated by adding 0.5 ml plasma to 0.5 ml acetonitrile. After centrifugation for 5 min at 13.000 rpm (IEC Micromax-centrifuge, Metric, Taastrup, Denmark), the acetonitrile was evaporated in vacuum. The supernatant was centrifuged again for 2 min at 13,000 rpm and the subsequent supernatant was divided into two fractions (*A* and *B*).

*Fraction A* was analyzed by applying a system previously described for the analysis of the content of metabolites formed from the

sugar analog FDG in tissue biopsies (4, 21). Briefly, the analysis was performed on a radio-HPLC system with online radioactivity detection applying a Phenomenex Sphereclone 5μ SAX 250 × 4.6 mm anion exchange column with 20 mM potassium phosphate buffer pH 7.3 as mobile phase and a flow rate of 0.8 ml/min. Only the radioactivity channel was recorded, and chromatograms were analyzed via commercial available chromatography software (Dionex Chromeleon 6.50).

*Fraction B* was analyzed for possible isomerization of FDGal to FDG. Analysis was performed by applying a Perkin-Elmer LC pump 200 (Titan) equipped with a Rheodyne 7125 injector and 100 μl PEEK injection loop, connected in series with a Dionex Carbopac PA1 column, a Dionex PEDII electrochemical detector and a sodium iodide scintillation detector of in-house design. The mobile phase was a sodium hydroxide solution (0.15 mmol/l) and the flow rate 0.5 ml/min. Chromatograms were analyzed with commercially available chromatography software (Dionex Chromeleon 6.50). Radio-HPLC fractions were collected with 0.5 min (Gilson FC 203B fraction collector, started with a delay of 3 min because of column void volume) and counted in a Canberra Packard Cobra II well counter. To check for FDG formation, every analyzed sample was spiked with both nonradioactive 2-fluoro-2-deoxygalactose and 2-fluoro-2-deoxyglucose and electrochemical detection was recorded together with the collection of fractions. Under the applied chromatographic conditions FDGal and FDG would be separated. FDGal eluted first, followed by FDG with difference of 0.8 min in retention time.

On the basis of aliquot, the recovery from radio-HPLC was higher than 90% for both *fractions A* and *B*.

### DATA ANALYSIS

Regions of interest were drawn in the liver using an image of the mean FDGal radioactivity concentrations from 10 to 90 min, carefully excluding large vessels by viewing the image side-by-side with the corresponding CO images (Ecat7 Software). The regions of interest were summed into a volume of interest that was transferred to the dynamic scan and a tissue TAC of the time course of the tissue concentration of radioactivity in that volume was extracted.

The flow-weighted dual-input concentration was calculated as:

$$c_{dual}(t) = \frac{F(t)_{HA}\, c(t)_{HA} + F(t)_{PV}\, c(t)_{PV}}{F(t)_{HA} + F(t)_{PV}} \qquad (1)$$

where $F(t)_{HA}$ and $F(t)_{PV}$ are the flow rates in HA and PV, respectively, and $c(t)_{HA}$ and $c(t)_{PV}$ are the radioactivity concentrations in the corresponding vessels at a given time, *t*.

The hepatic blood perfusion, Q (ml blood·min$^{-1}$·ml liver tissue$^{-1}$) was calculated as total flow (from the ultrasound transit-time flowmeters) divided by the wet liver weight and corrected for tissue density (1.07 g/ml; M. Sørensen, unpublished observation).

Whole blood concentrations of galactose and FDGal were used because no quantitatively important amount of galactose enters pig erythrocytes (22). The estimated clearances are hence in terms of per milliliter whole blood.

*FDGal kinetics from nonlinear regression analysis.* Figure 1 shows the two-tissue compartmental model of FDGal metabolism used to analyze data. The model was fitted to the PET data by nonlinear regression analysis using the flow-weighted dual input, $c_{dual}$ (*Eq. 1*). The PET camera records the sum of $q_1$, $q_2$, and $q_3$ (Fig. 1) where $q_1$ is defined as $c_{dual}$ $V_b$. The hepatic blood volume, $V_b$, was determined from the CO PET. Differential equations corresponding to the model in Fig. 1 are

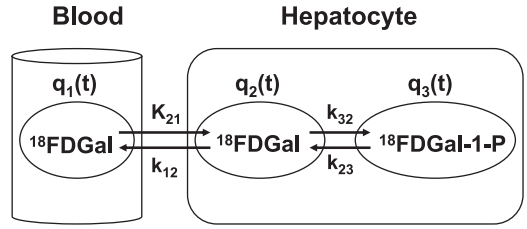


Fig. 1. The 2-tissue compartmental model of 2-[$^{18}$F]fluoro-2-deoxygalactose (FDGal) metabolism fitted to data (4k model). $q_1$, Pool of FDGal in sinusoidal blood compartment; $q_2$, intracellular pool of FDGal; $q_3$, intracellular pool of FDGal metabolites, primarily FDGal-1-phosphate. $K_{21}$, unidirectional clearance of blood FDGal into hepatocytes (ml blood·min$^{-1}$·ml liver tissue$^{-1}$); $k_{12}$, rate constant for backflux of FDGal from hepatocytes back to the systemic circulation (min$^{-1}$); $k_{32}$, rate constant of enzymatic conversion of FDGal to FDGal-1-phosphate by galactokinase (min$^{-1}$); $k_{23}$, rate constant for dephosphorylation of FDGal-1-P (min$^{-1}$). On the basis of initial fittings, $K_{21}$ was set equal to the hepatic blood perfusion, Q (see text for details). The parameter $k_{23}$ was ignored in the calculation of the net metabolic clearance of FDGal by galactokinase from linear representation of the data (3k model).

$$\begin{aligned} \dot{q}_2(t) &= K_{21}c_{dual}(t) - (k_{12} + k_{32})q_2(t) + k_{23}q_3(t) \\ \dot{q}_3(t) &= k_{32}q_2(t) - k_{23}q_3(t) \end{aligned} \qquad (2)$$

where the dots denote differentiation with respect to time, *t* (6). The differential equations (*Eq. 2*) were solved assuming no initial activity in the compartments. The model solution was fitted to data by optimizing the four model parameters $K_{21}$, $k_{12}$, $k_{32}$, and $k_{23}$ by nonlinear regression (33). The tracer is assumed to be in instantaneous spatial equilibrium in each compartment at each time point and the model ignores the development of concentration gradients of FDGal along the length of the sinusoids (37). Initial fittings gave $K_{21}$ values close to or even higher than the measured blood perfusion, Q (ml blood·min$^{-1}$·ml tissue$^{-1}$). In the final estimation of the kinetic parameters (Fig. 1) $K_{21}$ was therefore set equal to the measured average Q during the initial 2 min following the injection of FDGal to limit the number of estimated parameters (Table 1).

*Steady-state metabolic clearance of FDGal from linear representation of data.* Linear representation of data is used to yield a robust measure of the net metabolic clearance of tracer. In this representation, $M_1(t)/c_i(t)$ is plotted against $\theta(t)$ as (10, 39)

$$\frac{M_1(t)}{c_i(t)} = K^{FDGal}\theta(t) + V, \quad \theta(t) = \frac{\int_0^t c_i(t)dt}{c_i(t)} \qquad (3a)$$

where

$$K^{FDGal} = K_{21}\frac{k_{32}}{k_{12} + k_{32}}, \qquad V = V_0 + K_{21}\frac{k_{12}}{(k_{12} + k_{32})^2} \qquad (3b)$$

$M_1$ is the tissue concentration of radioactivity recorded by the PET camera, $c_i$ is the blood input concentration of FDGal, and $V_0$ is the vascular FDGal content divided by the inflow concentration. The other parameters correspond to those in Fig. 1. $K^{FDGal}$ is the slope of the asymptote fitted to linear repre-

Table 1. *Model results*

| Experiment | Arterial Galactose, mmol l blood$^{-1}$ | Results from Nonlinear Regression 4k Model (90 min, using $c_{dual}$) $K_{21}(=Q)$, ml·min$^{-1}$·ml$^{-1}$ | $k_{12}$, min$^{-1}$ | $k_{32}$, min$^{-1}$ | $k_{23}$, min$^{-1}$ | Results from Linear Regression 3k Model (40 min) $K_{dual}^{FDGal}$, ml·min$^{-1}$·l$^{-1}$ | $K_{arterial}^{FDGal}$, ml·min$^{-1}$·l$^{-1}$ | $E_{met}$ | $V_{max}^{Gal}$, μmol·min$^{-1}$·l$^{-1}$ |
|---|---|---|---|---|---|---|---|---|---|
| *1* | <0.01 | 0.965 | 0.376 (1.8) | 0.482 (2.5) | 0.021 (1.8) | 411.0 (2.4) | 403.5 (3.1) | 0.43 | n.d. |
| *2* | <0.01 | 1.054 | 0.277 (1.8) | 0.371 (2.7) | 0.020 (2.3) | 455.2 (2.6) | 431.5 (2.6) | 0.43 | n.d. |
| *3* | <0.01 | 0.787 | 0.349 (3.8) | 0.398 (6.2) | 0.013 (14.2) | 331.8 (1.4) | 293.3 (1.0) | 0.42 | n.d. |
| *4* | <0.01 | 1.076 | 1.215 (4.1) | 1.491 (4.6) | 0.018 (2.2) | 481.2 (2.1) | 441.4 (2.1) | 0.45 | n.d. |
| *5* | 0.49 | 0.499 | 0.401 (0.02) | 0.065 (0.03) | 0.000 (6.4) | 73.2 (0.2) | 70.0 (0.2) | 0.15 | n.d. |
| *6* | 0.62 | 0.594 | 0.987 (2.0) | 0.129 (4.2) | 0.004 (18.8) | 56.5 (0.4) | 55.9 (0.5) | 0.10 | n.d. |
| *7* | 3.06 | 0.853 | 1.011 (1.3) | 0.026 (9.7) | 0.004 (64.9) | 19.5 (0.9) | 18.7 (1.0) | 0.02 | 412 |
| *8* | 3.88 | 1.091 | 1.389 (1.2) | 0.030 (8.0) | 0.004 (51.4) | 21.8 (2.7) | 22.8 (2.5) | 0.02 | 584 |
| *9* | 6.60 | 0.853 | 1.251 (1.3) | 0.027 (10.5) | 0.007 (37.8) | 15.4 (2.3) | 16.6 (3.9) | 0.02 | 702 |
| *10* | 6.65 | 0.750 | 0.919 (0.3) | 0.018 (1.1) | 0.000 (76.5) | 15.2 (1.1) | 15.6 (5.4) | 0.02 | 701 |

Optimized values from kinetic fittings are given as estimates and standard errors of the estimates (percent). Standard errors or the estimates are based on the covariance matrix. The lower detection limit for arterial galactose is 0.01 ml/l blood. $K_{21}$, $k_{12}$, $k_{32}$, and $k_{23}$ are model parameters; $K_{21}$ was set equal to the perfusion, Q, in each experiment (ml blood·min$^{-1}$·ml tissue$^{-1}$). $K_{dual}^{FDGal}$ and $K_{dual}^{FDGal}$, net metabolic clearance of 2-[$^{18}$F]-fluoro-2-deoxygalactose with dual tracer or single arterial input, respectively. The net metabolic extraction fraction during quasi-steady-state metabolism, $E_{met}$, was calculated as $K_{dual}^{FDGal}/Q$ (*Eq. 4*). The maximal hepatic removal rate of galactose, $V_{max}^{Gal}$, was calculated from *Eq. 8a,* which is only applicable in cases with near-saturation kinetics, viz. *experiments 7–10*. In these cases the kinetics approximated saturation with 94–97%. n.d., Not determined.

sentation of data during quasi-steady state from 17.5 to 40 min after the injection of FDGal by using the measured $M(t)$ and $c_i$ (10, 39). For each pig we calculated $K_{dual}^{FDGal}$ using $c_{dual}$ as $c_i$ and $K_{arterial}^{FDGal}$ using the single arterial input as $c_i$ and compared the two values using a paired *t*-test. The linear regressions were solved by using orthogonal least squares that account for variance on both variables. $K^{FDGal}$ is an in vivo estimate of the net metabolic clearance of FDGal by galactokinase.

*Extraction fractions.* The extraction fraction, E, is related to the clearance and perfusion as

$$E = \frac{K}{Q} \tag{4}$$

where K is the clearance (ml blood·min$^{-1}$·ml tissue$^{-1}$) and Q is the perfusion. Inserting the initial unidirectional clearance, $K_{21}$, in *Eq. 4* gives the initial extraction fraction, $E_0^{FDGal}$, of the tracer and inserting the net metabolic clearance, $K_{dual}^{FDGal}$, gives the net metabolic extraction fraction, $E_{met}^{FDGal}$, of the tracer. $E_{met}^{FDGal}$ was used to evaluate the backflux of FDGal from hepatocyte to blood. If $E_{met}^{FDGal}$ is lower than unity this can be ascribed to a high rate constant for backflux ($k_{12}$) compared with the metabolic rate constant ($k_{32}$) since $K_{dual}^{FDGal} = K_{21}\, k_{32}/(k_{32}+k_{12})$ (*Eq. 3B*) and because $K_{21}$ was set equal to Q.

*Intrinsic clearance of FDGal.* The intrinsic clearance of FDGal was calculated as

$$\frac{V_{max}}{K_m} = -Q \ln (1 - E_{met}^{FDGal}) \tag{5}$$

which is applicable in the sinusoidal perfusion model and at approximately first-order kinetics (*experiments 1–4*) (22, 29).

*The analog effect.* Six of the animals had a constant infusion of galactose, which was started 75–90 min before the injection of FDGal and continued throughout the PET study. FDGal and galactose are both assumed to be substrates for the galactokinase. The clearance of FDGal (ml blood·min$^{-1}$·ml tissue$^{-1}$) is accordingly dependent on the respective Michaelis-Menten kinetics for both FDGal and the nonradioactive galactose, Gal, as well as the concentrations of the two substrates (6, 7):

$$\frac{v^{FDGal}}{c^{FDGal}} = \frac{V_{max}^{FDGal}}{C^{FDGal} + K_m^{FDGal}\left(1 + \dfrac{c^{Gal}}{K_m^{Gal}}\right)} \tag{6}$$

$v^{FDGal}$ is the removal rate of FDGal and $c^{FDGal}$ the blood concentration of FDGal. $V_{max}^{FDGal}$ is the maximum removal rate of FDGal and $V_{max}^{Gal}$ is the maximum removal rate of galactose. $c^{Gal}$ is the blood concentration of galactose. $K_m^{FDGal}$ is the Michaelis-Menten constant for FDGal and $K_m^{Gal}$ is the Michaelis-Menten constant for galactose. In each of these four cases $c^{Gal}/K_m^{Gal} \gg 1$. $c^{FDGal}$ was negligible because of the low amount of tracer injected (maximum 0.33 mmol). Consequently, *Eq. 6* is reduces to

$$\frac{v^{FDGal}}{c^{FDGal}} = \frac{V_{max}^{FDGal}}{c^{Gal}}\frac{K_m^{Gal}}{K_m^{FDGal}} \tag{7}$$

At high concentration of galactose, $c^{Gal}$, the net metabolic clearance, $K^{FDGal}$, in *Eqs. 3a* and *3b* is equal to $v^{FDGal}/c^{FDGal}$ and *Eq. 7* can be rewritten:

$$V_{max}^{Gal} = \alpha K^{FDGal} c^{Gal} \tag{8a}$$

where

$$\alpha = \frac{V_{max}^{Gal}/K_m^{Gal}}{V_{max}^{FDGal}/K_m^{FDGal}}. \tag{8b}$$

The constant α is a result of the galactokinase acting on FDGal and galactose simultaneously. From *Eq. 8B* it is seen that α is the ratio between the intrinsic clearance of galactose and that of FDGal.

The Michaelis-Menten relation for in vitro phosphorylation of galactose by the galactokinase enzyme is

$$v^{Gal} = V_{max}^{Gal}\frac{c^{Gal}}{K_m^{Gal} + c^{Gal}} \tag{9}$$

where $v^{Gal}$ is the removal rate of galactose. When $c^{Gal} > 10\, K_m^{Gal}$ then $V^{Gal}$ approximates $V_{max}^{Gal}$ with more than 90% and the

reaction is considered near saturated. $K_m^{Gal}$ for the pig liver galactokinase enzyme is 0.28 mmol/l (2) and at concentrations higher than 2.8 mmol/l the galactokinase reaction is accordingly near saturated (*experiments 7–10*). Because of the development of a concentration gradient along the length of the sinusoid in vivo (37), a minimum inlet galactose concentration of 3 mmol/l blood is required to ensure near-saturation along the whole sinusoid (22). In the following, when referring to approximately first-order kinetics, intermediate kinetics, and near-saturation kinetics, we hence refer to the kinetics of the nonradioactive substance, galactose, according to the arterial blood concentration of this. The kinetics of FDGal is always first order because of the low dose injected.

## RESULTS

Arterial blood concentrations of galactose ($c^{Gal}$) ranged from <0.01 to 6.65 mmol/l (Table 1). As mentioned, the reaction catalyzed by galactokinase is at near-saturation when $c^{Gal}$ >3 mmol/l (*experiments 7–10*).

Figure 2 shows an example of a PET image of the mean liver tissue concentration of radioactivity from 10 to 90 min. In each experiment the accumulation of radioactivity in the liver was very high compared with surrounding tissue. As demonstrated by the time courses of the concentrations of radioactivity in the liver tissue (Fig. 3), the hepatic accumulation of FDGal was lower in the pigs that received a constant IV infusion of galactose than in the pigs that received IV saline. Also, the initial vascular phase, in which the tracer bolus distributes in the tissue, became very prominent in the presence of galactose.

Radio-HPLC analysis of the blood samples showed that ~85–90% of the radioactivity in blood was unmetabolized FDGal. No fractions of FDGal metabolites, including FDG, were detected in any of the samples. There was a minor content of $^{18}$F-fluoride which indicates a minor defluorination of FDGal (Fig. 4). The amount of $^{18}$F-fluoride increased throughout the experiment and was ~8% in the last sample (90 min). In the late samples, there was a small fraction with a retention time between 12 and 14 min (up to 8% of total radioactivity), but because of the very low concentration of radioactivity at this time point this metabolite was not identified.

*FDGal kinetics from nonlinear regression analysis.* Figure 3 shows examples of fitting the model in Fig. 1 to data by nonlinear regression. Table 1 gives the individual kinetic rate constants for FDGal. $K_{21}$ was set equal to the perfusion, Q, in all experiments. The rate constant for metabolic conversion of FDGal metabolites, $k_{23}$, decreased distinctly with increasing $c^{Gal}$.

We initially compared the goodness of the fit using a kinetic model without a $k_{23}$ (3k model) with the goodness of fit using a model including a $k_{23}$ (4k model). The former assumes irreversible trapping of tracer whereas the latter allows for the reaction to be reversible. Visually, the 4k model yielded better fits to data than the 3k model and always yielded positive values of $k_{23}$ (Table 1). When evaluated according to the Akaike information criterion (1), the 4k model also had a tendency to yield lower scores compared with the 3k model, but the finding was not statistically significant ($P > 0.3$). Fitting a 4k model to data up to 40 min after tracer injection yielded estimates of $k_{23}$ not significantly different from zero in all of the experiments (mean value 0.003, 95% confidence interval −0.009–0.015). This formed the basis for applying a 3k model to data up to 40 min after injection of tracer.

*Steady-state metabolic clearance of FDGal.* The hepatic net metabolic clearance of FDGal was drastically reduced in experiments with high blood concentrations of galactose compared with the experiments with concentrations <0.01 mmol/l (Table 1, Fig. 5). $K_{dual}^{FDGal}$ calculated by using flow-weighted dual input was not statistically significantly different from $K_{arterial}^{FDGal}$ calculated by using the single arterial input (the mean difference was −0.0003 ml blood·min$^{-1}$·ml liver tissue$^{-1}$; 95% confidence interval −0.027–0.026).

*Extraction fractions.* Because $K_{21}$ was set equal to Q, the initial extraction fractions, $E_0^{FDGal}$, was unity in all experiments. The presence of nonradioactive galactose caused the net metabolic extraction fraction, $E_{met}^{FDGal}$, to drop from ~0.43 (approximately first-order kinetics) to 0.02 (near-saturation kinetics) (Table 1).

*Intrinsic clearance of FDGal, analog effect, and maximal hepatic removal rate of galactose.* The intrinsic clearance of the tracer was calculated from *experiments 1–4* (*Eq. 5*) and was 0.42 ml blood·min$^{-1}$·ml tissue$^{-1}$ (range 0.36–0.47). The intrinsic clearance of galactose is 2.91 ml plasma·min$^{-1}$·ml tissue$^{-1}$ (26). According to *Eq. 8B* this gives an α of 6.92 after correcting the intrinsic clearance in the present study for the hematocrit to get similar units. The maximal hepatic removal rates of galactose, $V_{max}^{Gal}$, calculated in the experiments with near-saturated kinetics, viz. *experiments 7–10*, was hence on average 600 μmol·min$^{-1}$·l$^{-1}$ tissue (range 412–702) (Table 1).


Fig. 2. PET image of the mean concentration of radioactivity in the liver (*experiment 4*) from 10–90 min after injection of FDGal (coronal slice). Max and Min on the color scale refer to tissue concentrations of radioactivity (kBq/ml liver tissue).

## DISCUSSION

The present study is the first in vivo PET study with estimation of kinetic parameters of galactose uptake and metabolism in pig liver using the galactose analog FDGal. The results have provided new insights into the dynamic behavior of galactose in the intact liver. Since galactose is not normally present in blood during fasting we were able to study the effect of a constant infusion of nonradioactive (cold) galactose on the FDGal kinetics. FDGal followed first-order kinetics because of the low amount injected (tracer dose). Near-saturation of the enzymatic system by nonradioactive galactose caused a strong competition between galactose and FDGal for the galactokinase, which affected the kinetics of FDGal significantly. This is illustrated in Fig. 3 and in Table 1, which shows the dramatic effect of galactose on the hepatic accumulation of FDGal. The decreased enzymatic removal of FDGal made the initial vas-

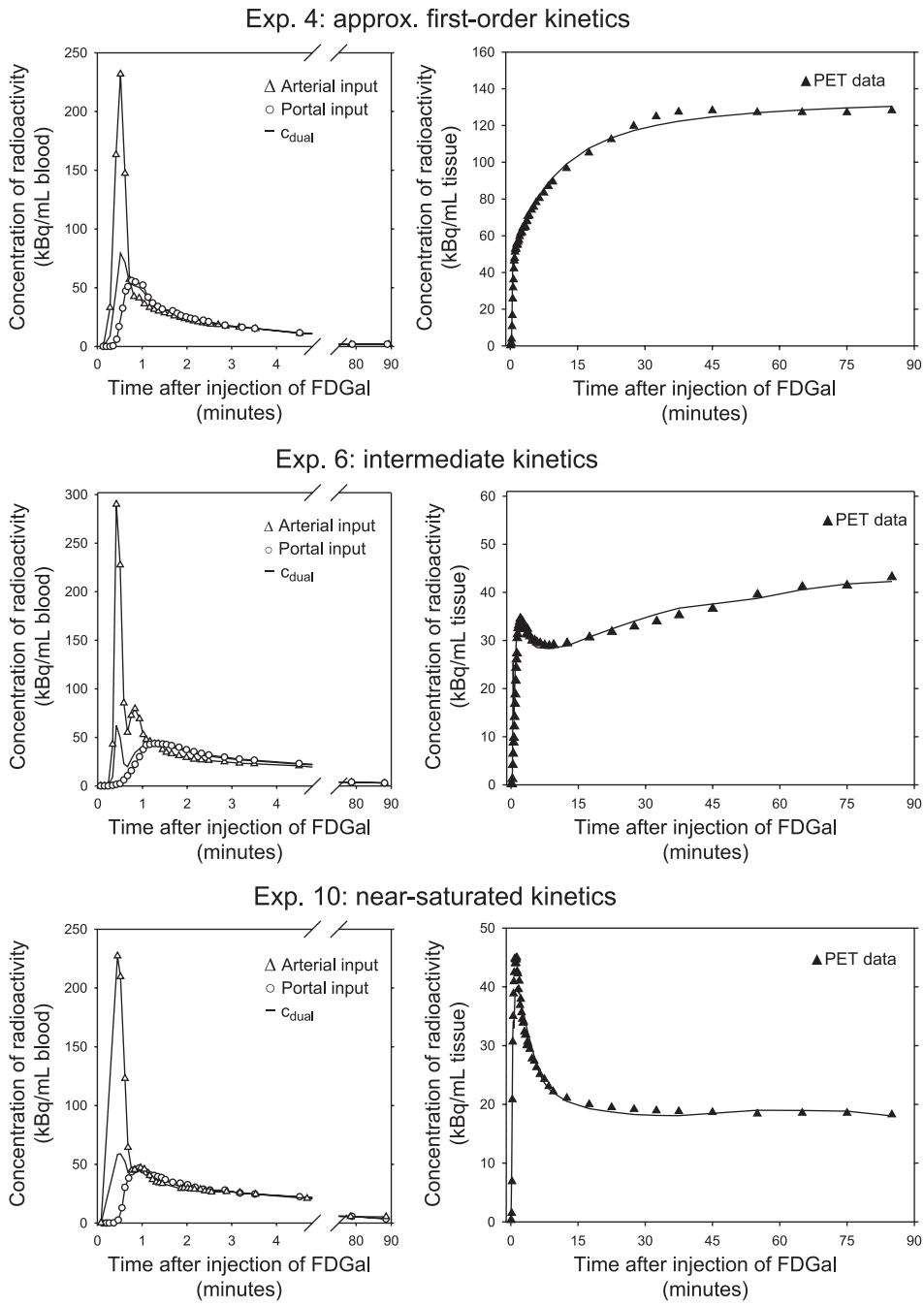


Fig. 3. Examples of time-activity curves (TACs) for blood and liver tissue from 3 experiments following an intravenous bolus injection of FDGal. Top row is from *experiment 4* (approximately first-order kinetics; arterial concentration of galactose <0.01 mmol/l), middle row is from *experiment 6* (intermediate kinetics; arterial concentration of galactose was 0.62 mmol/l), and bottom row is from *experiment 10* (near-saturated kinetics; arterial blood galactose was 6.65 mmol/l). Left column shows the blood curves. The blood TACs illustrate the distinct differences in shape between arterial, portal venous, and flow-weighted dual input within the initial 5 min following tracer injection. After the initial distribution of tracer, the concentration of radioactivity in the hepatic artery, $c_{art}$, is equal the flow-weighted dual input, $c_{dual}$. Right column shows corresponding liver tissue TACs (▲) with the 4k model fitted to data (solid line). The differences between the 3 tissue TACs were a direct effect of nonradioactive galactose in blood that decreased the hepatic accumulation of FDGal.

cular phase and distribution of tracer between plasma and hepatocytes (and interstitial space) very prominent. This initial phase was not as evident in the experiments with approximately first-order kinetics of galactose because of the high enzymatic removal of FDGal.

As a consequence of a very high permeability of the hepatocyte plasma membrane for both galactose and FDGal, we were unable to estimate the true rate constant for the unidirectional clearance, $K_{21}$. It was equal to or even higher than the blood perfusion Q, and since the operational rate constant cannot exceed the perfusion we set $K_{21}$ equal to Q. As a result of this, the initial extraction fraction, $E_0$, was unity in all experiments. This demonstrates a very high capacity of the hepatocyte membrane for transport of galactose from sinusoid to hepatocyte in agreement with the findings in dog livers by Goresky et al. (11), who used the multiple indicator dilution method. The net metabolic extraction fraction, $E_{met}^{FDGal}$ (Table 1), was lower than unity, which demonstrates that the backflux of galactose and FDGal from hepatocyte to blood was likewise high. The distribution of both FDGal and galactose across the hepatocyte plasma membrane can therefore be considered in steady-state shortly following a bolus injection of FDGal.

Administration of galactose strongly affected the hepatic accumulation of FDGal as reflected by the lower tissue concentrations of radioactivity compared with the experiments with no galactose infusion (Fig. 3). The rate constant for

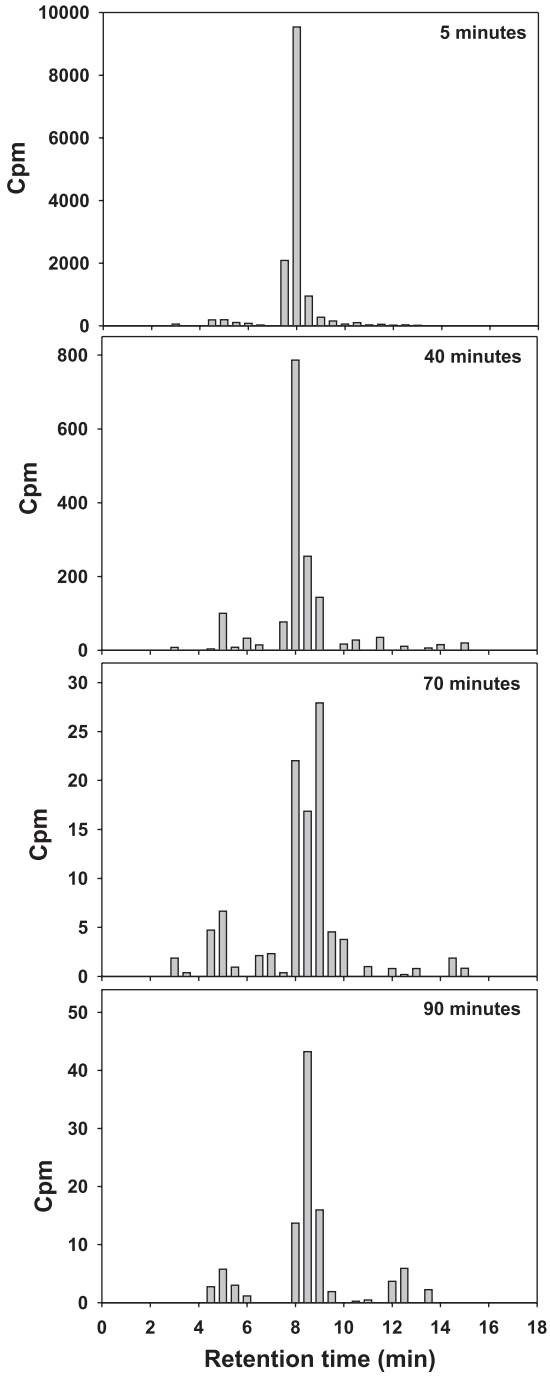


Fig. 4. Results from radio-HPLC (system B) from 4 plasma samples taken at 5, 40, 70, and 90 min after injection of FDGal. Diagrams show the relative amounts of unmetabolized FDGal and FDGal metabolites in blood. Unmetabolized FDGal was the main substance in blood throughout the experiment. See text for more details. Cpm, counts per minute.

enzymatic trapping of FDGal by hepatic galactokinase, $k_{32}$, decreased as the blood concentration of galactose, $c^{Gal}$, increased (Table 1). In accordance with this, the net metabolic clearance of FDGal decreased in experiments with galactose infusions compared with experiments without galactose infusion, verifying that galactose and FDGal are both phosphorylated by the galactokinase enzyme (Fig. 5 and Table 1). PET studies in rodents also found that galactose caused a decrease in hepatic accumulation of FDGal, but the kinetics of the underlying processes was not studied (9, 12, 19).

The distinct difference between the initial time course of blood TACs for arterial and the flow-weighted dual input (Fig. 3) demonstrates why the single arterial input cannot be used to estimate specific kinetic parameters for hepatic uptake and removal rates, which are sensitive to the changes in the initial data (36). There was no statistically significant difference between the quasi-steady-state parameters $K_{dual}^{FDGal}$ and $K_{arterial}^{FDGal}$, however. Any loss of FDGal in the prehepatic splanchnic area during quasi-steady-state metabolism would cause a systematic and significant difference between $c_{dual}$ and $c_{arterial}$ that subsequently would cause the $K_{arterial}^{FDGal}$ to be significantly lower than the $K_{dual}^{FDGal}$. When the $c_{arterial}$ and $c_{dual}$ for the entire study period were integrated, the two integrals did not differ from each other by more than 1%. Our results thus demonstrate no significant loss of FDGal in the PV drained viscera during quasi-steady-state metabolism. The feasibility of calculating the net metabolic clearance of FDGal using the single arterial input makes the method applicable for future human studies.

It may be noted that the concentration in *Eq. 8a*, $c^{Gal}$, is actually the amount of galactose available to the galactokinase enzyme, i.e., the concentration in the intracellular precursor pool as illustrated in Fig. 1. It can be assumed to equal the arterial plasma concentration at steady state because the distribution of FDGal between sinusoid and hepatocyte is very fast. The model applied to data was an "inlet equilibration model" that ignores the development of concentration gradients of FDGal along the length of the sinusoids (37). This had effect, however, only on the experiments with approximately first-order kinetics, in which cases the kinetic parameters were somewhat underestimated, because the true input is lower than the inlet concentration, $c_{dual}$. In the experiments with near-saturation kinetics the concentration gradients can be neglected because of the low difference between the inlet concentration and the outlet concentration (22).

When saturating the galactokinase enzyme with galactose, the effect on the net metabolic clearance of FDGal, $K^{FDGal}$, can be mathematically expressed as shown in *Eq. 6*. The galactokinase reaction is near saturated when $c^{Gal}$ is >3 mmol/l and then *Eq. 6* reduces to *Eq. 8a*, which shows that $V_{max}^{Gal}$ for galactose can be calculated from $K^{FDGal}$ and $c^{Gal}$ if corrected for the ratio between the intrinsic clearances for FDGal and galactose, viz. the constant $\alpha$. The hepatic $V_{max}^{Gal}$ in the four pigs with blood concentrations of galactose higher than 3 mmol/l (*experiments 7–10*) ranged from 412 to 702 $\mu mol \cdot min^{-1} \cdot l^{-1}$ tissue (Table 1). Corrected for liver tissue density (1.07 g/ml), the average calculated $V_{max}^{Gal}$ was 642 $\mu mol \cdot min^{-1} \cdot kg^{-1}$ liver (range 441–751 $\mu mol \cdot min^{-1} \cdot kg^{-1}$), which is similar to the $V_{max}^{Gal}$ determined in the intact pig liver by means of liver vein catheterization (550–950 $\mu mol \cdot min^{-1} \cdot kg^{-1}$ tissue) (26, 51).

The nonlinear regression analysis indicated that a dephosphorylation of FDGal-1-P occurs as expressed by the positive rate constant $k_{23}$, a reaction not normally expected to occur in hepatocytes. The positive $k_{23}$ values could be ascribed to limitations of our 4k model, which assumes only two intracellular compartments (Fig. 1). The true intracellular metabolism of FDGal is probably more complex, similar to the metabolism of FDG (4), with further conversion of FDGal-1-P into metabolites that might escape the hepatocytes. This escape of FDGal metabolites would be very slow and result in very low con-

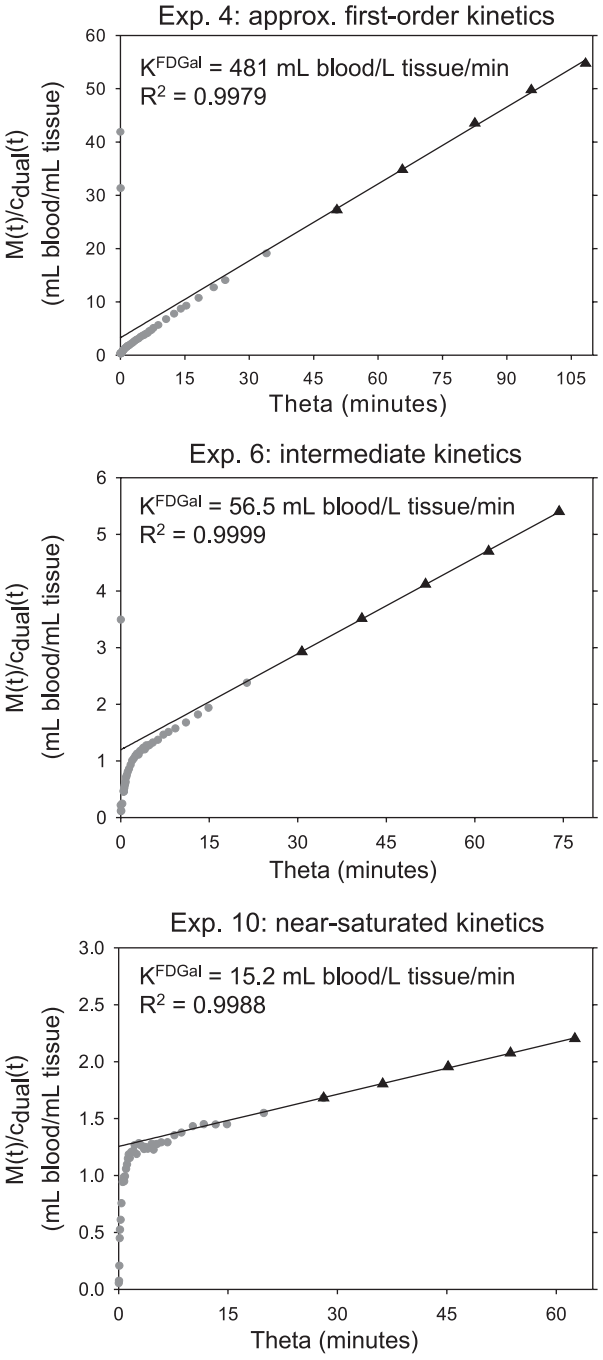


Fig. 5. Examples of linear representation of data up to 40 min after an intravenous bolus injection of FDGal. Top is from *experiment 4* (approximately first-order kinetics; arterial concentration of galactose <0.01 mmol/l), middle is from *experiment 6* (intermediate kinetics; arterial concentration of galactose was 0.62 mmol/l), bottom is from *experiment 10* (near-saturated kinetics; arterial blood galactose was 6.65 mmol/l). The slope of the fitted asymptote (solid line) is the net metabolic clearance of FDGal, $K^{FDGal}$, during quasi-steady-state metabolism (▲). Data up to 17.5 min (pre-quasi-steady-state) after injection are not included in the calculation (●). Note that each panel extends over the same experimental time (40 min) and that the abscissa is the theta time (*Eq. 3a*). M(*t*) is the tissue concentration of radioactivity measured by PET; $c_{dual}$, flow-weighted dual input.

centrations in peripheral blood to explain why we did not detect any FDGal metabolites in the blood samples. Another explanation could be that there actually might be galactose-1-phosphatase in the hepatocytes. Some enzymes have indeed been shown to be able to dephosphorylate galactose-1-phosphate (13, 38), but these enzymes have yet not been isolated from liver tissue. If present, it would take some time before enough FDGal-1-P is formed and hence substrate is available to the enzymes, similar to the delay hypothesis of the dephosphorylation of FDG-6-phosphate in brain (14). The enzymes might also be located in intracellular compartments that are not easily accessible for the FDGal-1-P (such as the endoplasmatic reticulum) which would cause a further time delay (8). Consequently, the $k_{23}$ is not showing its effect on the data until after some time. In support of this, when we fitted a 4k model to our data up to 40 min after injection the analysis yielded $k_{23}$ values not statistically significantly different from zero. Calculating the net metabolic clearance, $K^{FDGal}$, from linear representation of data up to 40 min after traces injection is therefore reasonable because the uptake and metabolism of FDGal up to this time point can be considered irreversible, which was also demonstrated by the very linear appearance of data in the graphical representation (Fig. 5). Analyzing the FDGal PET data by linear representation of data accordingly gives a good in vivo measure of the hepatic clearance of galactose by the galactokinase enzyme.

The constant α in *Eqs. 8a* and *8b* is a direct result of the different affinity of galactokinase for the two substrates galactose and FDGal. This phenomenon is well known in PET studies and is referred to as the lumped constant (LC). The LC accounts for the different affinity of the combined membrane transport and subsequent intracellular metabolism for two analogs. It has especially been discussed in PET studies of glucose metabolism using the glucose analog FDG (18, 30, 40, 50). Our study could not demonstrate any competitive inhibition of the hepatocyte plasma membrane transport for FDGal by galactose. The membrane transport can thus be ignored in the estimation of a LC for FDGal. However, the galactokinase enzyme has a much greater affinity for galactose than for FDGal, which in *Eq. 8b* is expressed in terms of the ratio between the two intrinsic clearances of the two substances. A ratio of 6.92 is quite high compared with the LC for FDG in pig liver, which in a recent study was estimated to be close to unity (18). The hepatic uptake of glucose is strictly regulated by factors such as insulin, however, which caused the LC to vary from 0.98 during hyperinsulinemia to 1.18 during fasting (18). Hepatic removal of galactose is not affected by insulin or glucose levels in blood (44) and neither is the uptake of FDGal (9), and α can therefore be assumed to be unaffected by such factors. Furthermore, since α is the ratio between the two intrinsic clearances of the FDGal and galactose, it is not concentration dependent.

The importance of including α in FDGal PET studies depends on the purpose of the studies. If one is interested in following the same patient over time, one could just calculate the maximal hepatic removal rate of FDGal, as discussed for FDG (30). If, however, the true metabolism of galactose is wanted, then the correct LC is important to know. With loss of functional liver mass, the total $V_{max}$ of galactokinase is reduced for both galactose and FDGal. This would probably not affect α since it is merely the ratio between the two intrinsic clearances.

The traditional GEC test, as developed by Tygstrup (47, 48), gives a good estimate of the whole liver's GEC. The test is, however, biased by a small but varying extrahepatic galactose

metabolism. Compared with this, the novel FDGal PET method presented in this study is not biased by any extrahepatic metabolism of galactose since it is based on three-dimensional imaging of the liver's galactose uptake. The PET method also makes it possible to explore whether there are regional differences in the hepatic GEC in patients with for example cirrhosis of the liver or primary liver tumors. In the present study of healthy pig livers there was no statistically significant regional variation, and since there are no good pig models for chronic hepatic pathophysiological conditions we were unable to include such studies.

*Conclusion.* By using advanced PET technology we were able to study specific rate constants for hepatic uptake and intracellular metabolism of galactose in anesthetized pigs with the galactose analog FDGal. The study yielded new insight into hepatic galactose kinetics ranging from first-order kinetics at low blood concentrations of galactose to near-saturation kinetics at high blood concentrations of galactose. The results showed that FDGal moves freely in and out of the hepatocytes because of a high capacity of the hepatocyte plasma membrane for galactose transport. The net metabolic flux of galactose ($\mu$mol galactose$\cdot$min$^{-1}\cdot$l$^{-1}$ liver) can be calculated from FDGal PET by using the single arterial input. When the galactokinase enzyme is near saturated by a high blood concentration of galactose, then the flux equals the maximal hepatic removal rate of galactose, $V_{max}^{Gal}$. We have thus established a method for estimation of hepatic kinetics of galactose and specifically for calculating the maximal hepatic removal rate of galactose in vivo using FDGal PET. This method may prove useful for studies of patients with different diseases of the liver.


## ACKNOWLEDGMENTS

The authors thank the excellent staff at the PET Center, Aarhus University Hospital.

## GRANTS

The study was supported by grants from The Danish Medical Research Council (22-02-0337), The Novo Nordisk Foundation, The A.P. Møller Foundation for the Advancement of Medical Science, The Korning Foundation, and The National Institute of Diabetes and Digestive and Kidney Diseases (Grant 1 R01 DK-074419-01).


## REFERENCES


1. **Akaike H.** A new look at the statistical model identification. *IEEE Trans Automat Control* AC-19: 716–723, 1974.
2. **Ballard FJ.** Purification and properties of galactokinase from pig liver. *Biochem J* 98: 347–352, 1966.
3. **Ballard FJ.** Kinetic studies with liver galactokinase. *Biochem J* 101: 70–75, 1966.
4. **Bender D, Munk OL, Feng HQ, Keiding S.** Metabolites of $^{18}$F-FDG and 3-*O*-$^{11}$C-methylglucose in pig liver. *J Nucl Med* 42: 1673–1678, 2001.
5. **Bender D, Sørensen M, Hansen SB, Mueller M, Hoepping A, Keiding S.** Nucleophilic production and dosimetry in pig of 2-[F-18]-2-deoxy-galactose. *J Nucl Med* 47, *Suppl* 1: 1868, 2006.
6. **Carson RE.** Tracer kinetic modeling in PET. In: *Positron Emission Tomography: Basic Science and Clinical Practice* (1st ed.), edited by Valk PE, Bailey DL, Townsend DW, and Maisey MN. London, UK: Springer-Verlag, 2003, p. 147–179.
7. **Dixon M, Webb EC.** *Enzymes* (3rd ed.). Bungay, UK: Longman, 1979.
8. **Fishman RS, Karnovsky ML.** Apparent absence of a translocase in the cerebral glucose-6-phosphatase system. *J Neurochem* 46: 371–378, 1986.
9. **Fukuda H, Matsuzawa T, Tada M, Takahashi T, Ishiwata K, Yamada K, Abe Y, Yoshioka S, Sato T, Ido T.** 2-Deoxy-2-[$^{18}$F]fluoro-D-galactose: a new tracer for the measurement of galactose metabolism in the liver by positron emission tomography. *Eur J Nucl Med* 11: 444–448, 1986.
10. **Gjedde A.** Calculation of cerebral glucose phosphorylation from brain uptake of glucose analogs in vivo: a re-examination. *Brain Res Rev* 257: 237–274, 1982.
11. **Goresky CA, Bach GG, Nedeau BE.** On the uptake of material by the intact liver. The transport and net removal of galactose. *J Clin Invest* 52: 991–1009, 1973.
12. **Grün BR, Berger U, Oberdorfer F, Hull WE, Ostertag H, Friedrich E, Lehmann J, Keppler D.** Metabolism and actions of 2-deoxy-2-fluoro-D-galactose in vivo. *Eur J Biochem* 190: 11–19, 1990.
13. **Gulavita SJ, Zhang LP, Dougherty JJ, Dain JA.** Galactose-1-phosphatase in rat brain. *J Neurochem* 57: 520–526, 1991.
14. **Hawkins RA, Miller AL.** Deoxyglucose-6-phosphate stability in vivo and the deoxyglucose method. *J Neurochem* 49: 1941–1960, 1987.
15. **Herold C, Berg P, Kupfal D, Becker D, Schuppan D, Hahn EG, Schneider HT.** Parameters of microsomal and cytosolic liver function but not of liver perfusion predict portal vein velocity in noncirrhotic patients with chronic hepatitis C. *Dig Dis Sci* 45: 2233–2237, 2000.
16. **Herold C, Heinz R, Niedobitek G, Schneider T, Hahn EG, Schuppan D.** Quantitative testing of liver function in relation to fibrosis in patients with chronic hepatitis B and C. *Liver* 21: 260–265, 2001.
17. **Holden HM, Rayment I, Thoden JB.** Structure and function of enzymes of the Leloir pathway for galactose metabolism. *J Biol Chem* 278: 43885–43888, 2003.
18. **Iozzo P, Jarvisalo MJ, Kiss J, Borra R, Naum GA, Viljanen A, Viljanen T, Gastaldelli A, Buzzigoli E, Guiducci L, Barsotti E, Savunen T, Knuuti J, Haaparanta-Solin M, Ferrannini E, Nuutila P.** Quantification of liver glucose metabolism by positron emission tomography: validation study in pigs. *Gastroenterology* 132: 531–542, 2007.
19. **Ishiwata K, Ido T, Imahori Y, Yamaguchi K, Fukuda H, Tada M, Matsuzawa T.** Accumulation of 2-deoxy-2-[$^{18}$F]fluoro-D-galactose in the liver by phosphate and uridylate trapping. *Int J Rad Appl Instrum Biol* 15: 271–276, 1988.
20. **Jepsen P, Vilstrup S, Sørensen HT, Ott P, Keiding S, Andersen PK, Tygstrup N.** Galactose elimination capacity and prognosis of patients with liver cirrhosis-a Danish registry-based cohort study with complete long-term follow-up (Abstract). *J Hepatol* 40, *Suppl* 1: 69A, 2004.
21. **Kaarstad K, Bender D, Bentzen L, Munk OL, Overgaard J, Keiding S.** Metabolic fate of 2-[$^{18}$F]fluoro-2-deoxy-D-glucose in mice bearing C3H mammary or squamous cell (SCCVII) carcinoma. *J Nucl Med* 43: 940–947, 2002.
22. **Keiding S, Johansen S, Winkler K, Tønnesen K, Tygstrup N.** Michaelis-Menten kinetics of galactose elimination by the isolated perfused pig liver. *Am J Physiol* 230: 1302–1313, 1976.
23. **Keiding S, Johansen S, Tønnesen K.** Kinetics of alcohol inhibition of galactose elimination in perfused pig liver. *Scand J Clin Lab Invest* 37: 487–494, 1977.
24. **Keiding S, Chiarantini E.** Effect of sinusoidal perfusion on galactose elimination kinetics in perfused rat liver. *J Pharmacol Exp Ther* 205: 465–470, 1978.
25. **Keiding S, Vilstrup H, Hansen L.** Importance of flow and hematocrit for metabolic function in perfused rat liver. *Scand J Clin Lab Invest* 40: 355–359, 1980.
26. **Keiding S, Johansen S, Winkler K.** Hepatic galactose elimination kinetics in the intact pig. *Scand J Clin Lab Invest* 42: 253–259, 1982.
27. **Keiding S.** Galactose clearance and liver blood flow. *Gastroenterology* 94: 477–481, 1988.
28. **Keiding S, Johansen S, Tygstrup N.** Galactose removal kinetics during hypoxia in perfused pig liver: reduction of $V_{max}$, but not of intrinsic clearance $V_{max}/K_m$. *Eur J Clin Invest* 20: 305–309, 1990.
29. **Keiding S, Sørensen M.** Hepatic removal kinetics: importance for quantitative measurements of liver function. In: *Textbook of Hepatology: From Basic Science to Clinical Practice* (3rd ed.), edited by Benhamou JP, Dufour JF, Blei A, Friedman S, Reichen J, Ginès P, Rizzetto M, Valla DC, and Zoulim F. Oxford, UK: Blackwell, 2007, p. 468–478.
30. **Krohn KA, Muzi M, Spence AM.** What is in a number? The FDG lumped constant in the rat brain. *J Nucl Med* 48: 5–7, 2007.
31. **Kurz G, Wallenfels K.** D-Galactose, UV-Test mit Galactose-dehydrogenase. In: *Methoden der Enzymatischen Analyse*, edited by Bergmeyer HU. Weinheim, Germany: Verlag Chemie, 1970, p. 1241–1244.
32. **Lindskov J, Ranek L, Tygstrup N, Winkler K.** Splanchnic galactose uptake in patients with cirrhosis during continuous infusion. *Clin Physiol* 3: 179–185, 1983.
33. **Marquardt DW.** An algorithm for least-squares estimation of non-linear parameters. *J Soc Ind Appl Math* 11: 431–441, 1963.

34. **Merkel C, Gatta A, Zoli M, Bolognesi M, Angeli P, Iervese T, Marchesini G, Ruol A.** Prognostic value of galactose elimination. *Dig Dis Sci* 36: 1197–1203, 1991.
35. **Merkel C, Marchesini G, Fabri A, Bianco S, Bianchi G, Enzo E, Sacerdoti D, Zoli M, Gatta A.** The course of galactose elimination capacity in patients with alcoholic cirrhosis: possible use as a surrogate marker for death. *Hepatology* 24: 820–823, 1996.
36. **Munk OL, Bass L, Roelsgaard K, Bender D, Hansen SB, Keiding S.** Liver kinetics of glucose analogs measured in pigs by PET: importance of dual-input blood sampling. *J Nucl Med* 42: 795–801, 2001.
37. **Munk OL, Keiding S, Bass L.** Capillaries within compartments: microvascular interpretation of dynamic positron emission tomography data. *J Theor Biol* 225: 127–141, 2003.
38. **Parthasarathy R, Parthasarathy L, Vadnal R.** Brain inositol monophosphatase identified as a galactose 1-phosphatase. *Brain Res* 778: 99–106, 1997.
39. **Patlak CS, Blasberg RG, Fenstermacher JD.** Graphical evaluation of blood-to-brain transfer constants from multiple-time uptake data. *J Cereb Blood Flow Metab* 3: 1–7, 1983.
40. **Phelps ME, Huang SC, Hoffman EJ, Selin C, Sokoloff L, Kuhl DE.** Tomographic measurements of local cerebral glucose metabolic rate in humans with (F-18)2-fluoro-2-deoxy-D-glucose: validation of method. *Ann Neurol* 6: 371–388, 1979.
41. **Ranek L, Andreasen PB, Tygstrup N.** Galactose elimination capacity as a prognostic index in patients with fulminant liver failure. *Gut* 17: 959–964, 1976.
42. **Ranek L, Lindskov J, Tygstrup N, Winkler K.** Splanchnic galactose uptake in patients with cirrhosis following single injection. *Clin Physiol* 3: 173–178, 1983.
43. **Schmidt LE, Ott P, Tygstrup N.** Galactose elimination capacity as a prognostic marker in patients with severe acetaminophen-induced hepatotoxicity: 10 years' experience. *Clin Gastroenterol Hepatol* 2: 418–424, 2004.
44. **Sparks JW, Lynch A, Glinsmann WH.** Regulation of rat liver glycogen synthesis and activities of glycogen cycle enzymes by glucose and galactose. *Metabolism* 25: 47–55, 1976.
45. **Sørensen M, Keiding S.** Positron emission tomography of the liver. In: *Textbook of Hepatology: From Basic Science to Clinical Practice* (3rd ed.), edited by Benhamou JP, Dufour JF, Blei A, Friedman S, Reichen J, Ginès P, Rizzetto M, Valla DC, and Zoulim F. Oxford, UK: Blackwell, 2007, p. 561–566.
46. **Timson JT, Reece RJ.** Sugar recognition by human galactokinase. *BMC Biochem* 4: 16–23, 2003.
47. **Tygstrup N.** Determination of the hepatic elimination capacity (Lm) of galactose by single injection. *Scand J Clin Lab Invest Suppl* 18: 118–125, 1966.
48. **Tygstrup N.** Effect of sites of blood sampling in determination of the galactose elimination capacity. *Scand J Clin Lab Invest* 37: 333–338, 1977.
49. **Walker DG, Khan HH.** Some properties of galactokinase in developing rat liver. *Biochem J* 108: 169–175, 1968.
50. **Wienhard K.** Measurement of glucose consumption using [(18)F]fluorodeoxyglucose. *Methods* 27: 218–225, 2002.
51. **Winkler K, Henriksen JK, Tygstrup N.** Hepatic, renal and total body galactose elimination in the pig. *Am J Physiol Gastrointest Liver Physiol* 265: G9–G14, 1993.